ELSEVIER

Journal of Biomechanics 37 (2004) 457–470

JOURNAL OF BIOMECHANICS

www.elsevier.com/locate/jbiomech
www.JBiomech.com

Wave propagation in a model of the arterial circulation

J.J. Wang*, K.H. Parker

Physiological Flow Studies Group, Department of Bioengineering, Imperial College of Science, Technology and Medicine, London SW7 2AZ, UK

Accepted 2 September 2003

Abstract

The propagation of the arterial pulse wave in the large systemic arteries has been calculated using a linearised method of characteristics analysis to follow the waves generated by the heart. The model includes anatomical and physiological data for the 55 largest arteries adjusted so that the bifurcating tree of arteries is well matched for forward travelling waves. The peripheral arteries in the model are terminated by resistance elements which are adjusted to produce a physiologically reasonable distribution of mean blood flow. In the model, the pressure and velocity wave generated by the contraction of the left ventricle propagates to the periphery where it is reflected. These reflected waves are re-reflected by each of the bifurcations that they encounter and a very complex pattern of waves is generated. The results of the calculations exhibit many of the features of the systemic arteries, including the increase of the pulse pressure with distance away from the heart as well as the initial decrease and then the large increase in the magnitude of back flow during late systole going from the ascending aorta to the abdominal aorta to the arteries of the leg. The model is then used to study the effects of the reflection or absorption of waves by the heart and the mechanisms leading to the incisura are investigated. Calculations are carried out with the total occlusion of different arterial segments in order to model experiments in which the effects of the occlusion of different arteries on pressure and flow in the ascending aorta were measured. Finally, the effects of changes in peripheral resistance on pressure and velocity waveforms are also studied. We conclude from these calculations that the complex pattern of wave propagation in the large arteries may be the most important determinant of arterial haemodynamics.

Keywords: Homodynamics; Multiple waves reflection; Aortic transfer function

1. Introduction

The method of characteristics has previously been applied to the study of waves in the arteries by a number of authors (Skalak, 1972; Stettler et al., 1981; Stergiopulos et al., 1992). These studies can be grouped loosely into two approaches: highly idealised models which are concerned primarily with the propagation of waves in single vessels and very complex models which have attempted to predict the detailed behaviour of the arterial system. In the more complex models, it is difficult to ascribe cause to effect in the interpretation of the results of the numerical simulations. That is, it is impossible to say whether a particular feature of the results is due primarily to one or another of the several complexities of the model.

In this study, we have taken a slightly different approach to the modelling of waves in the arteries. In order to study the influence of the complex branching geometry of the arterial system on its haemodynamics, we have used a linearised form of the general solution of the one-dimensional flow equations with highly idealised cardiac function but a fairly realistic model of the anatomy of the largest arteries. By including only this one complexity into our model, we are confident that any complexities in the results of our calculations are due to the interaction of the simple input wave with the reflections and re-reflections arising from the complex geometry of the large arteries. We then alter the model parameters to explore the effects of individual features of our model on arterial pressure and velocity waveforms. We do not suggest that the results of our calculations provide a realistic model of arterial haemodynamics, but we do believe that the results demonstrate that many of the features of flow in the arteries can be ascribed to the effects of wave reflections.

*Corresponding author. Current address: Cardiovascular Research Group, Departments of Medicine and Physiology and Biophysics, University of Calgary, Calgary, Canada.

0021-9290/$ - see front matter © 2003 Elsevier Ltd. All rights reserved.
doi:10.1016/j.jbiomech.2003.09.007

Wave behaviour in the arteries has primarily been studied using the impedance method which also presumes linearity. The earliest comparable study was by Taylor (1966) who calculated the input impedance of two random networks of vessels with eight generations. There was no attempt to model a realistic arterial system. More recent studies have used more realistic models of the arterial system in their impedance calculations (Westerhof and Noordergraaf, 1970; Avolio, 1980; O'Rourke and Avolio, 1980; Stergiopulos et al., 1992). Indeed, we use the data collected by Westerhof and Noordergraaf and Stergiopulos et al. as the basis of our arterial model. The impedance method has also been applied to models of the pulmonary circulation (Milnor, 1989) and to a model based upon measurements of a cast of a right coronary artery (Zamir, 1998). All of these studies, while comparable to this work, are carried out in the frequency domain of Fourier analysis and thus lack the immediacy of the temporal analysis presented here. Also, impedance analysis is intrinsically linear whereas the method which we present can incorporate various non-linearities.

In the theory section, we give a very brief outline of the theoretical basis of our calculations and the algorithms we used. The details are available in Wang (1997). We then calculate the pressure and velocity waveforms at different locations in the arterial system in response to a simple, half-sinusoidal left ventricular contraction. The model is then used to study (i) the role of reflections from the heart, (ii) the effect of complete occlusion of the aorta at different locations and (iii) the effects of changes in peripheral resistance on the arterial pulse waveforms. Whenever possible, the results of our calculations are compared with relevant experimental observations.

2. Theory

2.1. The method of characteristics

The behaviour of blood in the arterial system is simulated as a one-dimensional, incompressible flow in elastic tubes. The governing equations for the pressure, P, and mean velocity, U, are hyperbolic and can be solved by the method of characteristics (Anliker et al., 1971; Skalak, 1972; Parker and Jones, 1990). The solution shows that any disturbance introduced into the artery will generate pressure and velocity waves that will propagate with the characteristic velocities $U \pm c$, where c is the local wave speed which is a function of the local distensibility of the artery D

$$c = \frac{1}{\sqrt{\rho D}},$$

where $D \equiv (1/A)\mathrm{d}A/\mathrm{d}P$, where A is the cross-sectional area of the artery and ρ is the density of blood. When the wave speed is greater than the mean velocity, as is the case in the arteries, one wave propagates downstream, taken as the positive direction, and the other upstream.

In a uniform artery when viscous effects are negligible, there is a simple relationship between the change in pressure, $\mathrm{d}P$, and velocity, $\mathrm{d}U$, across any wavefront

$$\mathrm{d}P = \pm \rho c \, \mathrm{d}U.$$

This relationship is usually known as the water hammer equation (Allieve, 1909) which can be derived using conservation of mass and momentum across the wave (Jones et al., 1994). We note that there is no assumption about periodicity and that a wave of any waveform, including discontinuities such as shock waves, will propagate along these characteristic directions.

2.2. Arterial model

The typical structure of large arteries is bifurcations with few, if any, trifurcations and no anastomoses in conduit arteries (Stergiopulos et al., 1992). The bifurcating tree structure extends to the very small arteries in most parts of the body, although there are exceptions such as the kidney, liver, head, hand and foot where there are interconnections. Thus, the large arterial system can be properly represented as a bifurcating tree. For our calculations, we have adapted a realistic human arterial tree which contains 55 large arteries (Fig. 1) using data collected by Westerhof et al. (1969) giving the length, diameter, wall thickness and elastic modulus for the 55 largest arteries of a normal adult human (Table 1). Using this data, we have calculated the wave speed of each segment using the Moens–Korteweg equation $c = \sqrt{Eh/2\rho R}$ where E is the Young's modulus and R is the radius of the vessel. The calculated wave speeds are included in Table 1. The terminal vessels in the model are terminated by resistance vessels through which the flow is determined by the local pressure and the resistance, R_p. The peripheral resistances, also given in Table 1, are chosen to give a physiologically reasonable distribution of mean flow throughout the model (Stergiopulos et al., 1992).

2.3. Reflections

The two types of reflections that must be considered in our model are those caused by the bifurcations and those generated in the high-resistance vessels at the ends of the terminal segments in our model. The reflection coefficients, defined as the ratio of the change in pressure across the reflected wave $\mathrm{d}P_0$ to that of the incident wave ΔP_0, for a bifurcation are

$$R \equiv \frac{\mathrm{d}P_0}{\Delta P_0} = \frac{Y_0 - Y_1 - Y_2}{Y_0 + Y_1 + Y_2},$$

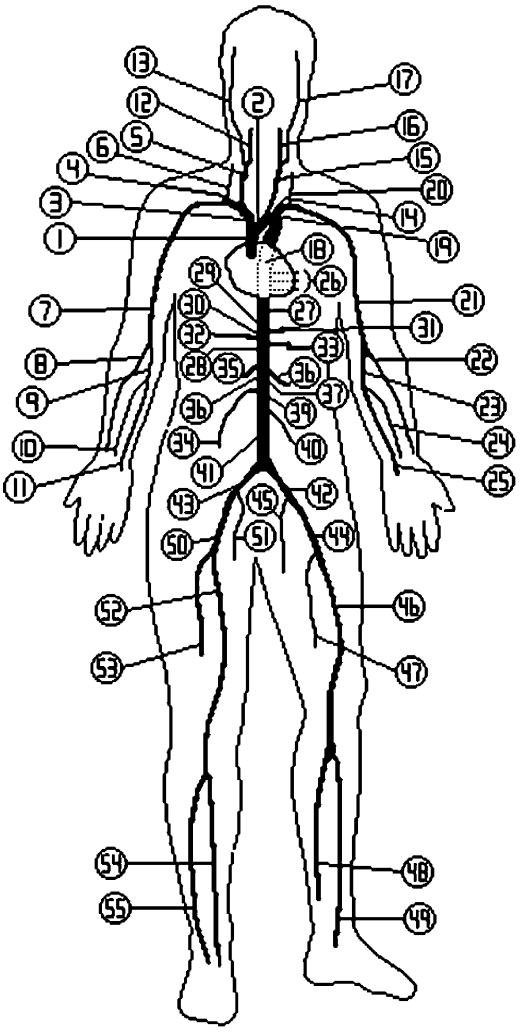

Fig. 1. The arterial model used in the calculation. This model was originally introduced by Westerhof et al. (1969) and contains data for diameter, length, wall thickness and Young's modulus for the 55 largest arteries (after Stergiopulos et al., 1992).

where $i = 0, 1, 2$ refer to the parent and two daughter vessels and $Y_i \equiv A_i/\rho c_i$ is the characteristic admittance of the ith vessel where A_i is the cross-sectional area. The transmission coefficient is $T = 1 + R$. Both the reflection and transmission coefficients at the junction depend upon the area and wave speed of each segment. If there is no reflection, $R = 0$, the junction is called 'well matched'. We note that this equation is valid for both forward and backward waves if the parent and daughter branches are determined relative to the wave rather than morphologically. Thus, a single bifurcation will have different reflection coefficients for waves approaching it in the three different vessels. This directional sensitivity of the reflection coefficient means that a junction that is well matched for forward waves can cause substantial reflections for backward waves (Hardung, 1952).

Calculating the reflection coefficients for the different bifurcations from the data collected by Westerhof et al. (1969) and Stergiopulos et al. (1992), we found that the data resulted in relatively large reflections coefficients for several of the junctions in the model. For example, the junction between the thoracic aorta I (segment 18) and the intercostal and the thoracic aorta II (segments 26 and 27) have a 50% decrease in area which results in a reflection coefficient $R \approx 0.25$. These reflections tended to obscure the effects of the reflections from the peripheral segments and so we decided to adjust the radii of the vessels to ensure that our model system was well matched for forward travelling waves. This was done by holding the parent vessel radius constant and increasing or decreasing the radii of both daughter vessels by the same fraction until $R = 0$. Table 1 includes the adjusted radii and the wave speeds calculated from them with the original radii and wave speeds given in brackets. Similarly, we found that the symmetry in the original data for the length of the arteries in the legs resulted in simultaneous reflections from each of the legs which resulted in unwanted interactions between reflected waves and so we somewhat arbitrarily increased the length of each artery in the right leg by 1 mm. The problem of simultaneous reflections from the arms did not arise because they are not symmetric.

For the resistances at the end of each terminal artery, the reflection coefficient depend upon the peripheral resistance, R_p (Lighthill, 1978):

$$R_T \equiv \frac{dP}{\Delta P} = \frac{R_P - \rho c}{R_P + \rho c}.$$

The values for the terminal reflection coefficients, R_T, are included in Table 1.[1]

2.4. The method of calculation

The method of characteristics outlined above does not make any assumptions about linearity. Indeed, the solution of the full, non-linear equations of one-dimensional flow is one of the advantages of the method. There are two principal non-linearities in that solution: the characteristic directions depend upon the velocity of the blood and the wave speed can be a function of pressure. Both of these non-linearities can be incorporated into the method, but in this study we have chosen to concentrate our attention on the effects of the complex geometry of the arteries and so we will assume that both of these non-linearities have a negligible effect, i.e. $c =$ constant in each arterial segment and $U \ll c$. We plan to explore the non-linear effects in a subsequent publication.

With this assumption of linearity, it is possible to apply the concept of the transfer function to the analysis

[1] The use of R_P as peripheral resistance and R_T as terminal reflection coefficient is unfortunate nomenclature, but one that is forced upon us by standard usage.

Table 1
Physiological data used in the model based upon the original data collected by Westerhof et al. (1968) and Stergiopulos et al. (1992)

No.	Name of segment	l (cm)	r (cm)	h (cm)	E (10^6 Pa)	c (m/s)	R_P (10^9 Pa s/m)
1	Ascending aorta	4.0	1.470 (1.470)	0.163	0.4	4.67 (4.67)	—
2	Aortic arch I	2.0	1.263 (1.120)	0.126	0.4	4.43 (4.70)	—
3	Brachiocephalic	3.4	0.699 (0.620)	0.080	0.4	4.47 (5.03)	—
4	R. subclavian I	3.4	0.541 (0.423)	0.067	0.4	4.93 (5.58)	—
5	R. carotid	17.7	0.473 (0.370)	0.063	0.4	5.11 (5.78)	—
6	R. vertebral	14.8	0.240 (0.188)	0.045	0.8	8.58 (9.69)	6.01
7	R. subclavian II	42.2	0.515 (0.404)	0.067	0.4	5.05 (5.71)	—
8	R. radius	23.5	0.367 (0.174)	0.043	0.8	6.78 (9.85)	5.28
9	R. ulnar I	6.7	0.454 (0.215)	0.046	0.8	6.31 (9.16)	—
10	R. interosseous	7.9	0.194 (0.091)	0.028	1.6	10.64 (15.54)	84.3
11	R. ulnar II	17.1	0.433 (0.203)	0.046	0.8	6.45 (9.43)	5.28
12	R. int. carotid	17.6	0.382 (0.177)	0.045	0.8	6.80 (9.99)	13.9
13	R. ext. carotid	17.7	0.382 (0.177)	0.042	0.8	6.57 (9.65)	13.9
14	Aortic arch II	3.9	1.195 (1.070)	0.115	0.4	4.35 (4.59)	—
15	L. carotid	20.8	0.413 (0.370)	0.063	0.4	5.47 (5.78)	—
16	L. int. carotid	17.6	0.334 (0.177)	0.045	0.8	7.27 (9.99)	13.9
17	L. ext. carotid	17.7	0.334 (0.177)	0.042	0.8	7.02 (9.65)	13.9
18	Thoracic aorta I	5.2	1.120 (1.000)	0.110	0.4	4.39 (4.65)	—
19	L. subclavian II	3.4	0.474 (0.423)	0.066	0.4	5.23 (5.53)	—
20	L. vertebral	14.8	0.203 (0.180)	0.045	0.8	9.32 (9.91)	6.01
21	L. subclavian II	42.2	0.455 (0.403)	0.067	0.4	5.38 (5.71)	—
22	L. radius I	23.5	0.324 (0.174)	0.043	0.8	7.21 (9.85)	5.28
23	L. ulnar I	6.7	0.401 (0.215)	0.046	0.8	6.71 (9.16)	—
24	L. interosseous	7.9	0.172 (0.091)	0.028	1.6	11.32 (15.54)	84.3
25	L. ulnar II	17.1	0.383 (0.203)	0.046	0.8	6.87 (9.43)	5.28
26	intercoastals	8.0	0.317 (0.200)	0.049	0.4	5.51 (6.93)	1.39
27	Thoracic aorta II	10.4	1.071 (0.675)	0.100	0.4	4.28 (5.39)	—
28	Abdominal aorta I	5.3	0.920 (0.610)	0.090	0.4	4.38 (5.38)	—
29	Celiac I	2.0	0.588 (0.390)	0.064	0.4	4.62 (5.68)	—
30	Celiac II	1.0	0.200 (0.200)	0.064	0.4	7.93 (7.93)	—
31	Hepatic	6.6	0.458 (0.220)	0.049	0.4	4.58 (6.61)	3.63
32	Gastric	7.1	0.375 (0.180)	0.045	0.4	4.85 (7.00)	5.41
33	Splenic	6.3	0.386 (0.275)	0.054	0.4	5.24 (6.21)	2.32
34	Sup. mensenteric	5.9	0.499 (0.435)	0.069	0.4	5.21 (5.58)	0.93
35	Abdominal aorta II	1.0	0.843 (0.600)	0.080	0.4	4.32 (5.12)	—
36	L. renal	3.2	0.350 (0.260)	0.053	0.4	5.45 (6.33)	1.13
37	Abdominal aorta III	1.0	0.794 (0.590)	0.080	0.4	4.45 (5.16)	—
38	R. renal	3.2	0.350 (0.260)	0.053	0.4	5.45 (6.33)	—
39	Abdominal aorta IV	10.6	0.665 (0.580)	0.075	0.4	4.70 (5.04)	—
40	Inf. mesenteric	5.0	0.194 (0.160)	0.043	0.4	6.60 (7.26)	6.88
41	Abdominal aorta V	1.0	0.631 (0.520)	0.065	0.4	4.50 (4.95)	—
42	R. com. iliac	5.9 (5.8)	0.470 (0.368)	0.060	0.4	5.00 (5.66)	—
43	L. com. iliac	5.8	0.470 (0.368)	0.060	0.4	5.00 (5.66)	—
44	L. ext. iliac	14.4	0.482 (0.320)	0.053	0.8	6.57 (8.06)	—
45	L. int. iliac	5.0	0.301 (0.200)	0.040	1.6	10.21 (12.53)	7.94
46	L. femoral	44.3	0.361 (0.259)	0.050	0.8	7.37 (8.71)	—
47	L. deep femoral	12.6	0.356 (0.255)	0.047	0.8	7.20 (8.51)	4.77
48	L. post. tibial	32.1	0.376 (0.247)	0.045	1.6	9.69 (11.96)	4.77
49	L. ant. tibial	34.3	0.198 (0.130)	0.039	1.6	12.44 (15.35)	5.59
50	R. ext. iliac	14.5 (14.4)	0.482 (0.320)	0.053	0.8	6.57 (8.06)	—
51	R. int. iliac	5.0 (5.0)	0.301 (0.200)	0.040	1.6	10.21 (12.53)	7.94
52	R. femoral	44.4 (44.3)	0.361 (0.259)	0.050	0.8	7.37 (8.71)	4.77
53	R. deep femoral	12.7 (12.6)	0.356 (0.255)	0.047	0.8	7.20 (8.51)	—
54	R. post. tibial	32.2 (32.1)	0.375 (0.247)	0.045	1.6	9.71 (11.96)	4.77
55	R. ant. tibial	34.4 (34.3)	0.197 (0.130)	0.039	1.6	12.46 (15.35)	5.59

The wave speed for each segment is calculated from the Moens–Korteweg equation and the data in the preceding columns. As explained in the text, the radii were adjusted from the original data (given in brackets) so that all of the bifurcations were well matched for forward waves. The wave speed based on the original radii are also given in brackets.

of waves in the arteries. For any linear system the output, $O(t)$, can be written as the convolution of the transfer function of the system, $H(t)$, with the input, $I(t)$, $O(t) = H(t) \otimes I(t)$, where $\otimes$ denotes the convolution operator. A convenient way to determine the transfer function is to measure the response of the system to a

unit pulse, $\delta(t)$, where $\delta(0)=1$ and $\delta(t)=0$ for $t\neq 0$, since $O(t)=H(t)\otimes\delta(t)=H(t)$.

In our problem, the unit pulse is simply a wave of amplitude 1 entering the arterial system at $t=0$. The transfer function is the response of the arterial system to this input which can be determined by tracking this wave through the multiple transmissions and reflections in the arterial system.

When we try to understand wave propagation in the arterial system by following each wave, there are three possible difficulties:

(1) At each bifurcation, it is not necessary for the two daughter vessels to have equal properties and so it is possible that one pulse wave has gone through several segments before the other finishes traversing one.

(2) Two waves originating from the same junction may go through the same vessels but in different sequence. These two waves will then coalesce into a single summation wave. The number of 'duplicate' paths increases combinatorially with the number of segments.

(3) The reflections and transmissions in the arterial system are unlimited so that some waves may never return to the origin. Therefore, there is no end for the computation.

To solve these problems, we adopt a new concept, the 'tree of waves', and introduce a numbering method for the arterial tree suitable for the computation. Each wave will generate three waves when it encounters a bifurcation; one reflected and two transmitted waves. Thus, the tree of waves is a trifurcating tree in which the index denotes the location of the wave in the arterial system and backward waves are denoted by a negative index. The structure of the arterial system is a bifurcating tree, so a binary system is suitable for the numbering of the branches. The ascending aorta is the root of the tree and is denoted as 1, its daughter vessels, the aortic arch and brachiocephalic artery are assigned as 2 (2×1) and 3 ($2\times 1+1$) and so on. Thus, segment N (not a terminal segment) will have daughter vessels $2N$ and $2N+1$. If N is in a terminal segment, it generates only the wave $-N$. A backward travelling wave $-N$ will generate a backward transmitted wave $-N/2 \bmod 1$ (the smallest integer greater than $-N/2$), a forward transmitted wave $N+1$ (if N is even) or $N-1$ (if N is odd) and a forward reflected wave N. Each backward wave can generate three waves except those travelling back to the ascending aorta, -1. If the heart acts as an absorber, the wave will terminate. If the heart acts as a total reflector, it will behave like a terminal artery with a reflection coefficient of unity. This tree of waves model successfully overcomes the problem of unlimited reflections and allows us to follow waves that traverse the same path in different sequences.

The number of waves grows exponentially with time. It is clearly impossible to record all of the waves that are generated in a bifurcating system and fortunately it is unnecessary since many of the waves become very small in amplitude. In our calculation, we choose a threshold and neglect all the waves whose amplitude relative to the input is less than the threshold. We have taken the threshold as both 10^{-3} and 10^{-4} and have chosen 10^{-3} as the threshold in the calculations shown here since there is no discernible difference in the waveforms generated using these two thresholds.

The algorithm used to find the transfer function by calculating the response of the system to a unit pulse simply tracks the waves, generation by generation, on the tree of waves until no waves with amplitude greater than the threshold remain. This transfer function is then used to calculate the response of the system to the more realistic half-sinusoid input condition.

3. Results

The model has been used to calculate the pressure and velocity waveforms from the ascending aorta to the femoral artery in response to an idealised waveform generated by the left ventricle, a single half-sinusoid of 300 ms duration. Since we are interested only in the resultant waveforms, all results are normalised with respect to the input wave using the diastolic pressure as the gauge pressure. The first results that we show are calculated assuming that the heart absorbs all waves which are reflected back to the root of the aorta. We then compare those results to those obtained when the heart acts as a total reflector. Using these two results, we model the effect of the aortic valve by treating the heart as an absorber during systole and as a reflector during diastole when the aortic valve is closed. These results also allow us to comment upon the effects of aortic regurgitation on flow in the more distal arteries.

The model is then used to calculate the response to a total occlusion of the aorta in an attempt to model the results of an experiment by Westerhof and his colleagues (Van den Bos et al., 1971). We then consider the effect of a decrease in peripheral resistance, comparable to that which is observed during exercise or in response to vasodilatory drugs, on the arterial waveforms. And finally, we look at the influence of the coronary arteries on the arterial waveforms.

3.1. Waveforms in the ascending Aorta

The pressure transfer function at the ascending aorta calculated using the data in the model used by Westerhof et al. (1969) and Stergiopulos et al. (1992) (Table 1, in brackets) is shown in Fig. 2a, where the heart is assumed to be an absorber. All the pulse waves apart from the input are reflections from the mismatched bifurcations or the terminal resistances. It is noted that there is a particularly large pulse wave at

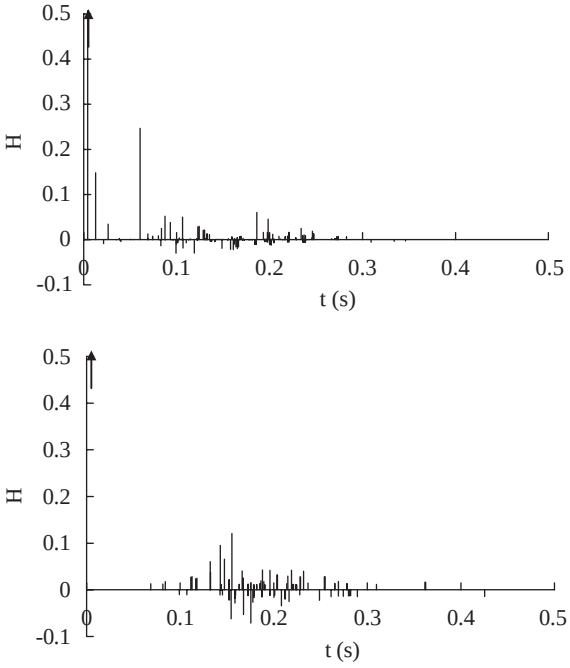

Fig. 2. The pressure transfer function calculated at the middle of the ascending aorta. The first line is the unit input pulse which is out of scale and denoted by an arrow. The rest of the peaks are the waves reflected by either unmatched bifurcations or terminal resistances. (a) Calculated using the data given by Westerhof et al. (1969). (b) Calculated using the well-matched model derived from this data. The large waves arriving before 0.1 s in (a) are reflections from poorly matched bifurcations in the original data.

$t = 0.05$, which is the reflection from the junction of the thoracic aorta I as mentioned above. The comparable transfer functions calculated using the well-matched model (Table 1) is shown in Fig. 2b. This model will be used in all of the calculations presented below.

The input waveform generated by ventricular systole is simply assumed to be a half-sinusoidal wave with a period of 0.3 s (the lower line in the middle panel of Fig. 3a) which is typical of the duration from the opening of the aortic valve to its closure. The pressure waveform (the upper line in middle panel of Fig. 3a) at the point of observation in the ascending aorta is the convolution of the input waveform with the pressure transfer function (left panel of Fig. 3). The velocity waveform (right panel of Fig. 3) is calculated by the same procedure but using the velocity transfer function. It is noted that the pressure transfer function is not the same as the velocity transfer function since the backward waves produce pulses which are opposite in sign.

The transformation of the pressure and velocity waveforms as they propagate along the main aortic trunk is one of the most striking features of wave propagation in the systemic arteries. The transfer functions and waveforms at five locations along the major arteries are shown in Fig. 3. The results show that the amplitude of pressure pulse increases distally, the amplitude of velocity decreases until the abdominal aorta and then begins to increase, the magnitude of the reverse flow also decreases and then begins to increase in the abdominal aorta. This behaviour is similar to that observed by McDonald (Nichols and O'Rourke, 1998). Note that the pulses in the transfer function are generally larger, more concentrated and closer to the input wave in the more distal arteries, which makes the pressure waveform steeper and the period of the pressure waveform shorter.

Backward compression waves coming to the point of observation from downstream increase the pressure but decrease the velocity, whereas backward expansion waves decrease the pressure but increases the flow. Conversely, forward compression waves arising from re-reflections from upstream sites increase both the pressure and velocity waveforms. This causes the increase in pressure and the decrease of the amplitude of both the forward velocity and the reverse flow as we move from the ascending aorta to the abdominal aorta, while further downstream the biggest waves are forward waves produced by reflections from branches upstream which travel without change through the intervening bifurcations which are well matched for forward waves.

3.2. The role of the heart in wave reflection

Frank (1899, 1905) and Hamilton (1944) first suggested that waves reflected from the heart might generate a standing wave in the arterial system. O'Rourke (1967) and McDonald (1974) rejected the possibility of standing waves in the arterial system from their experiments. But Nichols and O'Rourke (1998) again suggested as a result of their experiments that the heart valve should make some contribution to the pressure and velocity waveform.

In order to study the changes in the waveforms caused by the heart, we also made calculations assuming the heart is a total reflector, $R = 1$. The results are shown in Fig. 4 together with the previous results calculated assuming the heart is a total absorber, $R = 0$ (the lighter line). Several characteristics shown in these figures deserve comment:

(1) The gap between the pressure waveforms for a reflecting and absorbing heart is approximately the same through all the segments. That is because the systemic arteries are well matched for forward waves so that the waves reflected by the heart will propagate without reflection to the terminal segments.

(2) The velocity waveform is approximately the same as the input and there is almost no flow after the 0.3 s in the ascending aorta (Fig. 4b). When the heart is a reflector, the waves coming back from the periphery are reflected with a change in sign in the velocity, which leads to a cancellation of the velocity waveform, but with the same sign in the pressure, which leads to an

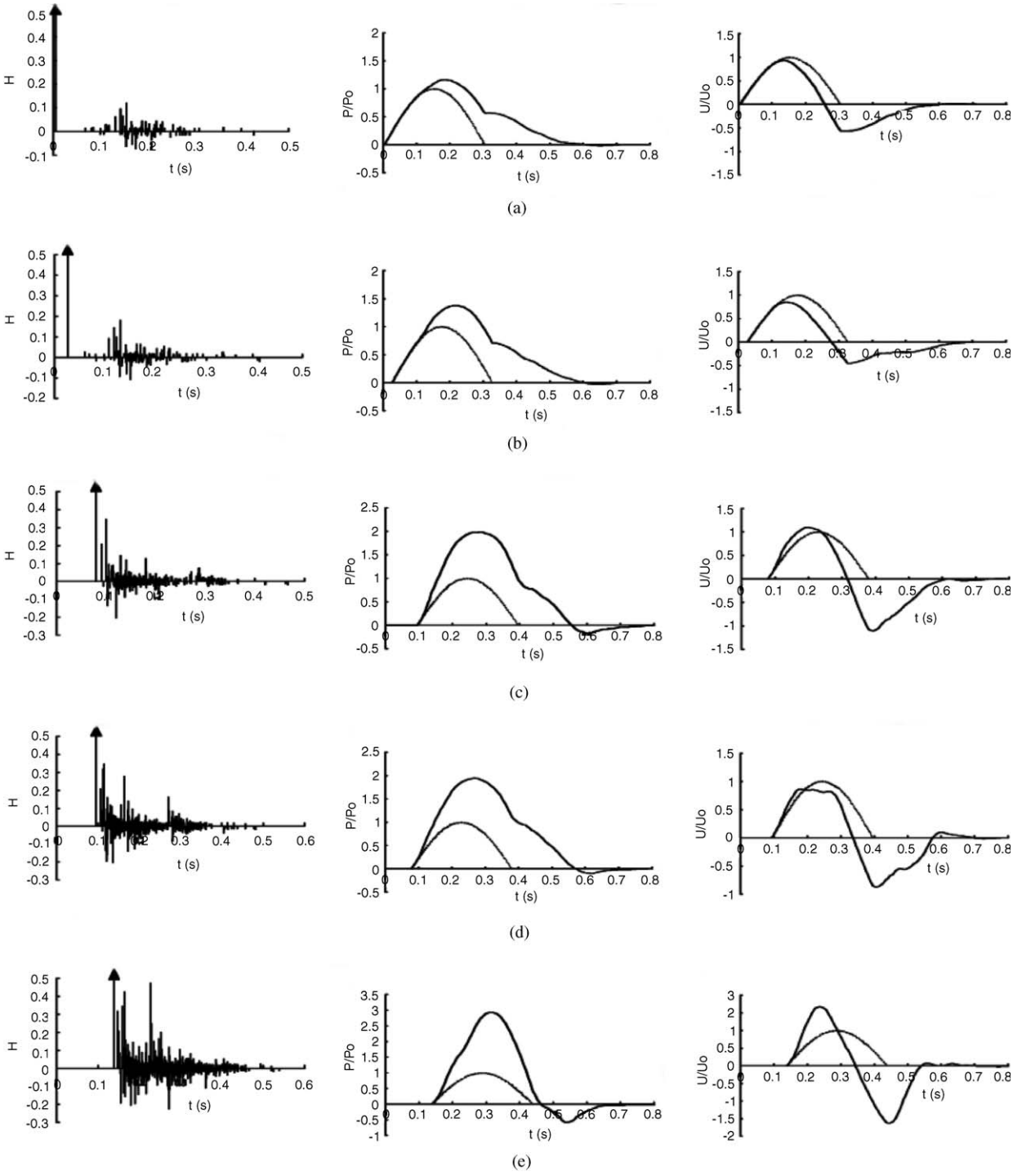

Fig. 3. The pressure transfer function (left), pressure waveform (middle) and velocity waveform (right) at five locations in the arterial system (a) ascending aorta (segment 1), (b) thoracic aorta I (segment 18), (c) abdominal aorta IV (segment 39), (d) left common iliac artery (segment 42) and (e) left femoral artery (segment 46). The pressure waveform is the convolution of the pressure transfer function and the aortic input which is simply assumed to be a half-sinusoidal wave (the dotted line). The velocity is calculated similarly using the velocity transfer function which differs from the pressure transfer function depending upon the direction of the waves.

amplification of the pressure waveform. Thus, the input becomes the only component left in the velocity waveform and the pressure waveform is amplified. In the aortic arch, some waves are transmitted through the brachiocephalic artery as forward waves without matched backward waves to cancel them, and so the flow is not strictly zero.

(3) A second 'hump' appears in the velocity waveform at the thoracic aorta I segment, where a larger lag between the waves reflected from the heart and

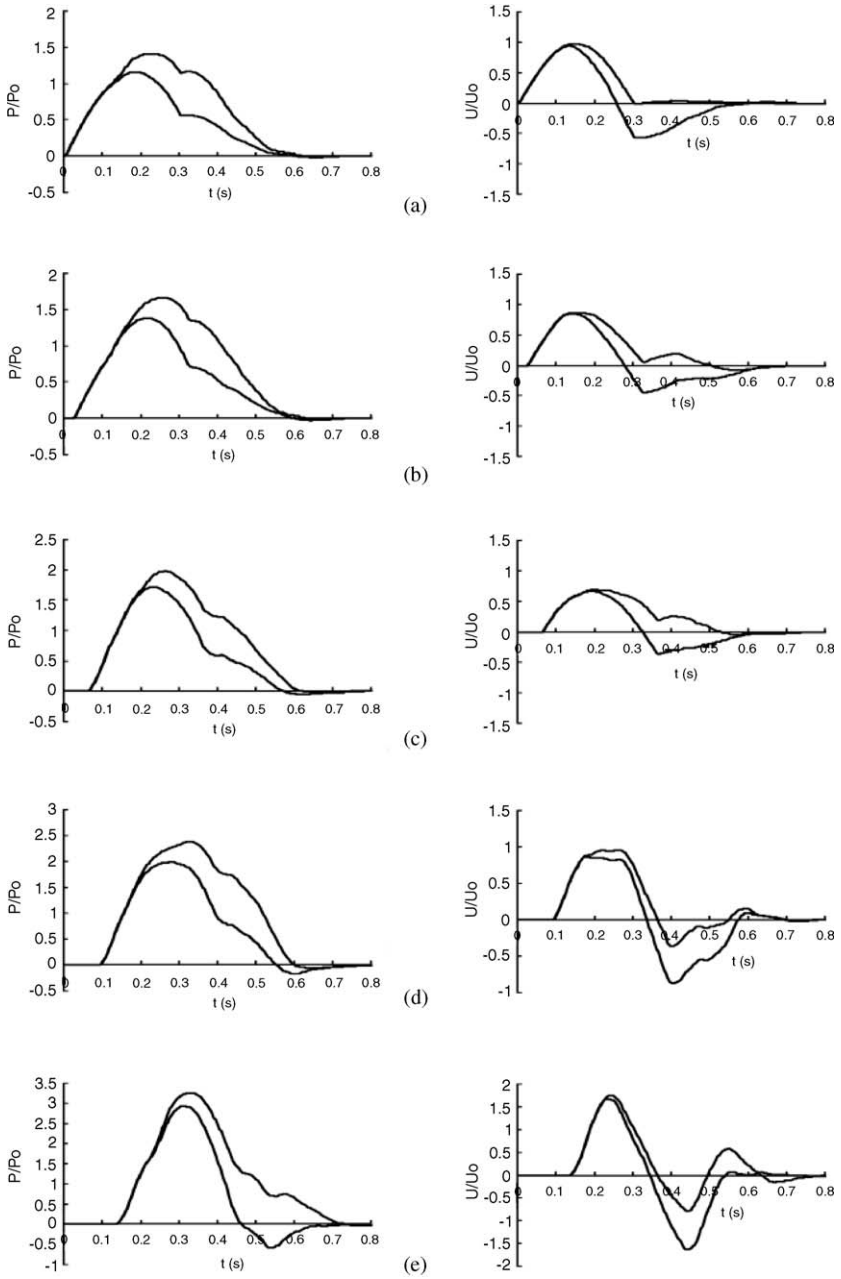

Fig. 4. Pressure (left) and velocity (right) waveforms at five locations in the arterial system calculated when the heart acts as a reflector (upper lines) and as an absorber (lower lines): (a) ascending aorta (segment 1); (b) thoracic aorta I (segment 18); (c) abdominal aorta IV (segment (39); (d) left common iliac artery (segment 42) and (e) left femoral artery (segment 46).

peripherally reflected waves is expected. Also, some waves propagate directly from the resistances in the upper limbs and the head to the observation point, and they will not have any counterpart to cancel their effects.

One interesting pathological application of the study of waveforms contributed by the aortic valve is aortic valve regurgitation arising from failure of the aortic valve during diastole. Measurement of blood flow in the femoral artery of patients who suffer from aortic valve regurgitation shows that there is generally a much larger reverse flow during diastole than in normal subjects (M. Heinen, personal communication). Aortic valve regurgitation can be simulated by considering the heart as an absorber while the normal heart is simulated by a total reflector, and the result is shown in Fig. 4e. The amplitude of the reverse flow with aortic valve regurgitation (the lighter line) is almost the same in contrast to the normal case when the heart is a reflector where the magnitude of the reverse flow is much lower. This result suggests that the larger back flow seen in the

femoral arteries during diastole could be caused by the absence of the waves normally reflected by the aortic valve.

3.3. The incisura and diastolic wave

Normally there is an increase in pressure, that is accompanied by a sudden cessation of the flow in the ascending aorta immediately after the closure of the aortic valve. This pressure rise is called the incisura, which is characterised as the reaction of the aortic pressure to the closure of the aortic valve. Normally, the magnitude of the rise is between 6 and 10 mm Hg in humans, but sometimes it can be higher so that the pressure after the closure of the aortic valve is equal or larger than the peak systolic pressure.

The usual interpretation of the origin of the incisura is that the back flow which causes the closure of the aortic valve is suddenly halted by the closure of the aortic valve giving rise to a short positive pressure immediately after the closure of the valve (Guyton, 1981). It is sometimes asserted that this rise in pressure is due to the recovery of the kinetic energy of the reverse flow when the valve closes. This is not reasonable since the Bernoulli equation indicates that a reverse flow of 1 m/s is required to generate a 4 mm Hg increase in pressure. However, the pressure and velocity changes associated with elastic tube waves, given by the water hammer equation, are physiologically reasonable. We have, therefore, used the model to simulate the effect of aortic valve closure on pressure and flow in the ascending aorta.

In order to incorporate the aortic valve in our model, the reflection coefficient of the heart is simply classified as having three states: the first 300 ms when the valve is fully opened and the heart acts as absorber ($R = 0$), a 10 ms period during which the valve is closing when it is assumed that the reflection coefficient increases from 0 to 1 as a linear function of time, and the final state when the valve is closed and acts as a reflector ($R = 1$). We note that the time-varying nature of the reflection coefficient at the heart introduces a non-linearity into the problem, making the straightforward calculation of the waveform as a convolution of the input with a transfer function invalid. That is, the portion of a reflected wave arriving before the valve is closed will be absorbed while the latter part of the wave will be reflected. It is, therefore, necessary to include in the convolution calculation a factor for each wave arriving at the heart which depends upon the time of arrival and accounts for the partial absorption of the wave. For details of the calculation, see Wang (1997).

The pressure and velocity waveforms calculated with the closing aortic valve are shown in Fig. 5, where the input is a half-sinusoidal wave. Several distinct characteristics of the waveforms measured in vivo are reproduced by this model:

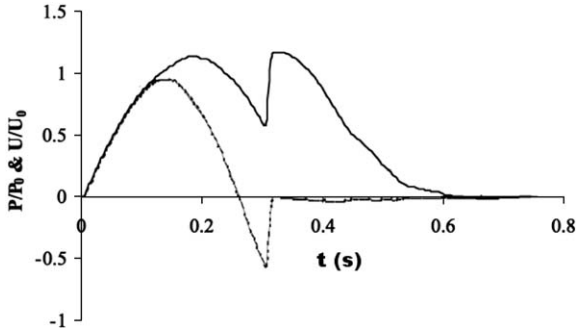

Fig. 5. The pressure (solid) and velocity (dotted) waveforms in the ascending aorta calculated assuming that the heart acts as an absorber during systole and as a reflector during diastole when the aortic valve is closed.

(1) The large pressure jump immediately after the closure of the aortic valve;
(2) the reverse flow halts immediately after the valve is closed;
(3) during the diastolic phase, apart from a very small oscillation, the flow velocity is nearly zero.

The zero flow after the closure of the aortic valve results from the cancellation of the changes in velocity produced by the backward waves and those reflected from the heart, which increases the pressure. Similar results are seen when the heart is a total reflector. This study indicates that the waves reflected by the aortic valve play an important role in determining the aortic waveforms. The magnified pressure waveform after the closure of the aortic valve seen in Fig. 5 has been observed in the human ascending aorta (M. Sugawara, personal communication), but generally the increase of pressure after the valve closed is less than we predict. An amplified pressure after the closure of the aortic valve is frequently found in kangaroos (Avolio et al., 1984; Nichols et al., 1986).

3.4. The effect of a complete occlusion of the aorta

The model can be extended to study the effects of an intervention such as an occlusion of an artery on the pressure and velocity waveforms. Van den Bos et al. (1971) performed a classic experiment in which they measured changes in pressure and flow in the canine ascending aorta when the aorta was occluded with a balloon catheter. The four sites of occlusion that they studied were the upper descending aorta, the aorta at the level of the diaphragm, the lower abdominal aorta and one of the iliac arteries. They analysed the results of their experiments using both an impedance analysis (Westerhof et al., 1973) and by separation of the

waveforms into forward and backward components (Westerhof et al., 1972; Stergiopulos and Westerhof, 1998). The experimental results have also been analysed using wave intensity analysis (Davies, 1994). When the occlusion is in the upper descending aorta, there is a large systolic wave and a prominent inflection point in the pressure waveform. The peak pressure is about twice as high as the control waveform. When the occlusion is at the level of the diaphragm, the inflection point is delayed and the peak pressure is only about 20% higher than the peak pressure of the control case. When the occlusion is in the abdominal aorta, the peak pressure decreases even more and the inflection point is delayed until late systole. When the occlusion is in one of the iliac arteries, there is no discernible difference between the occluded and control waveforms. The changes induced in the flow waveforms were relatively small compared to those of the pressure waveforms.

The four corresponding sites in our simulation of the human model are the thoracic aorta I (segment 18), abdominal aorta I (segment 28), abdominal aorta V (segment 41) and the right iliac artery (segment 42). The heart is assumed to act as an absorber. The results are shown in Fig. 6 and are compared with the control case in which there is no occlusion (thinner line). There are several important features:

(1) When the occlusion is located in the thoracic aorta I segment (Fig. 6a), the reflected waves arrive at the point of observation (middle of the ascending aorta) at 110 ms and forms a prominent inflection point. The peak pressure is about 40% higher than the control waveform. When the occlusion is in the abdominal aorta I segment (Fig. 6b), the reflected waves arrive at the point of observation later (130 ms), and the peak pressure decreases to about 20% higher than the control waveform. When the occlusion is in the abdominal V

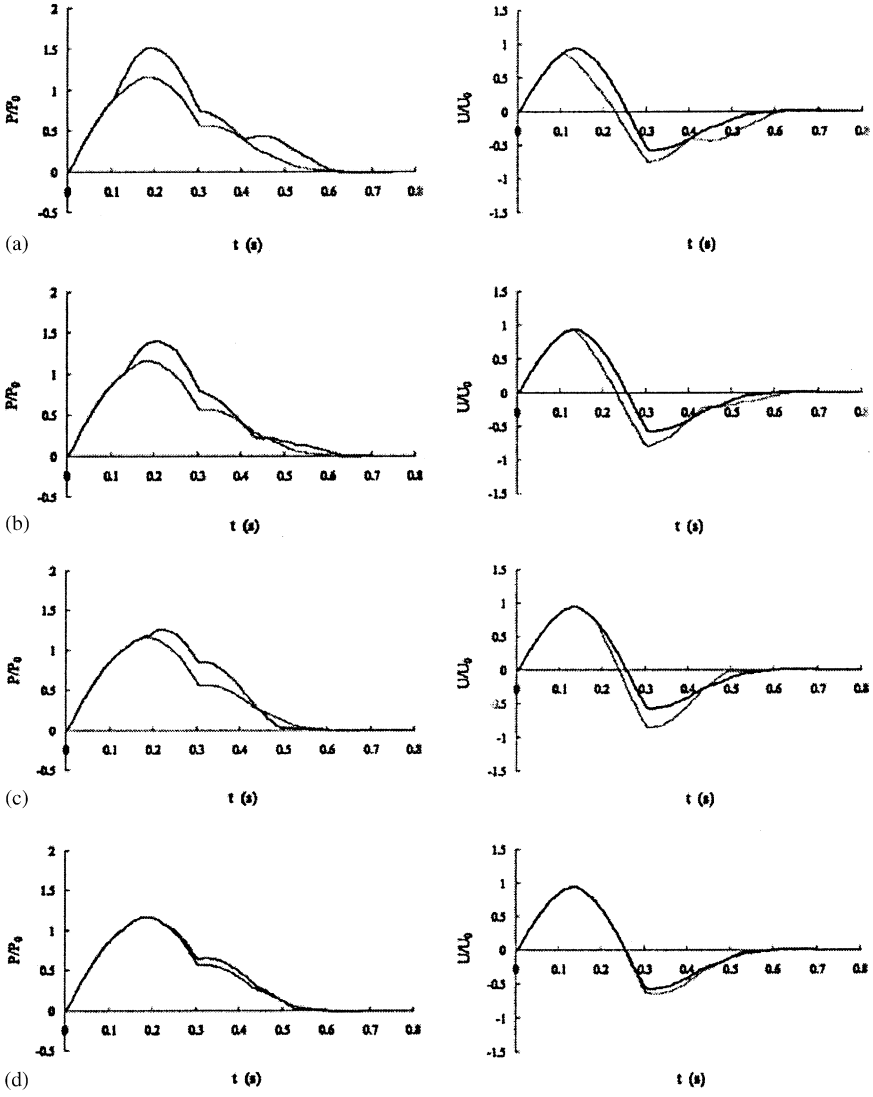

Fig. 6. The pressure (left) and velocity (right) waveforms in the ascending aorta with (solid) and without (dotted) a total occlusion of a peripheral artery: (a) occlusion of the upper descending aorta (segment 18); (b) occlusion of the aorta at the level of the diaphragm (segment 28); (c) occlusion of the abdominal aorta (segment 41) and (d) occlusion of the left iliac artery (segment 43).

segment (Fig. 6c), the reflected waves are even weaker and arrive at the point of observation even later. Finally, only a small deviation is found when the occlusion is in the left external iliac artery (Fig. 6d). The deviation of the velocity waveforms is relatively small in all cases.

The weakening of the reflected wave as the occlusion moves distally is due to the increased dispersal of the reflected wave caused by the mismatching for backward waves at each of the bifurcations which it encounters on its path back to the measurement site. For example, the magnitude of the reflected wave returning directly from the site of occlusion will be $\prod_{n=1}^{N} T_n$ where T_n is the transmission coefficient of the nth bifurcation and N is the number of bifurcations in the path between the occlusion and the site of measurement. When the occlusion is in the iliac artery, this product is so small that the effect of the direct reflection is not discernible. This fact was taken as evidence for no reflections in the systemic arteries by Peterson and Gerst (1956) who induced a pressure pulse in a dog's femoral artery and did not find any response in the ascending aorta. Latham et al. (1985) did a similar experiment with the bilateral occlusion of the femoral arteries of a dog and again did not find any significant difference in the pressure waveform measured in the ascending aorta.

(2) When the occlusion is in the thoracic aorta I segment, there is a significant pressure increase in the latter portions of the waveform. This gradually dies out when the occlusion is moved distally. The second pressure 'hump' is due to the group of waves arising from re-reflections by the occlusion. It should be remembered that there are no sources of dissipation in this model apart from the 'killing' of waves with magnitudes less than the threshold. The decrease in magnitude of the transmitted backward waves is because they are suffering from significant reflections due to the mismatching of the bifurcations for backward waves. These reflected waves propagate forward without loss through the system to the periphery or to the site of occlusion where they are again reflected as backward waves. As a result, the effect of an occlusion of a distal artery is not a single, easily identifiable wave, but a dispersed sequence of waves with ever decreasing magnitudes due to the ever increasing length of the path which they traverse before reaching the measurement site.

Normally, a sudden aortic occlusion or the increase in the peripheral resistance would induce a decrease of the ventricular output and an accumulation of blood in the ventricle in the first several beats. The enlargement of the ventricle due to the accumulation will increase the output of blood to make the system return to normal (Starling's law of the heart). This calculation assumes that the duration of the occlusion is short enough such that no physiological adjustment occurred in the cardiovascular system.

3.5. *The influence of terminal resistances and the coronary circulation on waveforms in the ascending aorta*

As a final application of the model, we calculate the variation of the waveforms in the ascending aorta under the influence of two factors: (1) the variation of terminal resistance and (2) the inclusion of the coronary circulation in the calculation.

Terminal resistance decreases with exercise. Murgo et al. (1981) measured aortic pressure and velocity in man at rest and during exercise and calculated the terminal resistance and characteristic impedance. During exercise, there is little change of the incisura and the backflow, but there is a distinct decrease in the pressure in diastole. The resistance falls about 35–55% during exercise, and the variation of the reflection coefficient of the terminal resistance falls about 10–20%.

To test the influence of the terminal resistances, the reflection coefficient of each terminal segment is decreased to 80% and then to 60% of the values in the table. The result is shown in Fig. 7. The waveforms are normalised by the peak value of the input waveform.

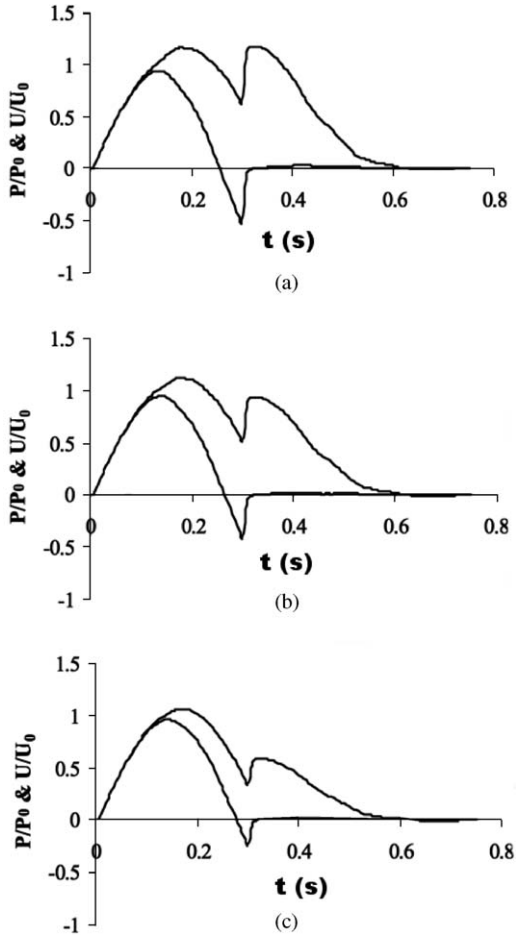

Fig. 7. The pressure (upper) and velocity (lower) waveforms in the ascending aorta calculated for decreasing terminal resistances: (a) control case; (b) 80% of control and (c) 60% of control.

As expected, when the terminal resistance decreases, the amplitude of the pressure decreases, and the decrease is greatest in late systole and diastole. Concurrently, the amplitude of the velocity increases and there is less reverse flow in late systole. In all cases, there is zero flow after the closure of the aortic valve.

The coronary circulation, which supplies the blood to the heart, has been neglected in our model calculations. However, it may have a prominent influence on the waveforms, particularly in the ascending aorta, especially in the diastolic phase. The right and left coronary arteries have their origin in the aorta directly above two of the cusps of the aortic valve. The branches of the coronary artery in the myocardium are compressed during each systole, so that the coronary blood flow is interrupted and even reverses in early systole. The coronary flow is restored when the stress in the ventricle wall decreases below the pressure in the arteries, but flow is only restored fully during diastole. About 80% of coronary flow occurs in the diastolic phase at basal heart rates (Levick, 1992). About 5% of the cardiac output goes to the coronary circulation, so that 4% of the total cardiac output flows into the coronary circulation during the diastolic phase. This is large enough to influence the waveforms in the ascending aorta. Therefore, the reflection coefficient of the heart, which incorporates the coronary circulation, may not be unity after the valve closes as we have previously assumed.

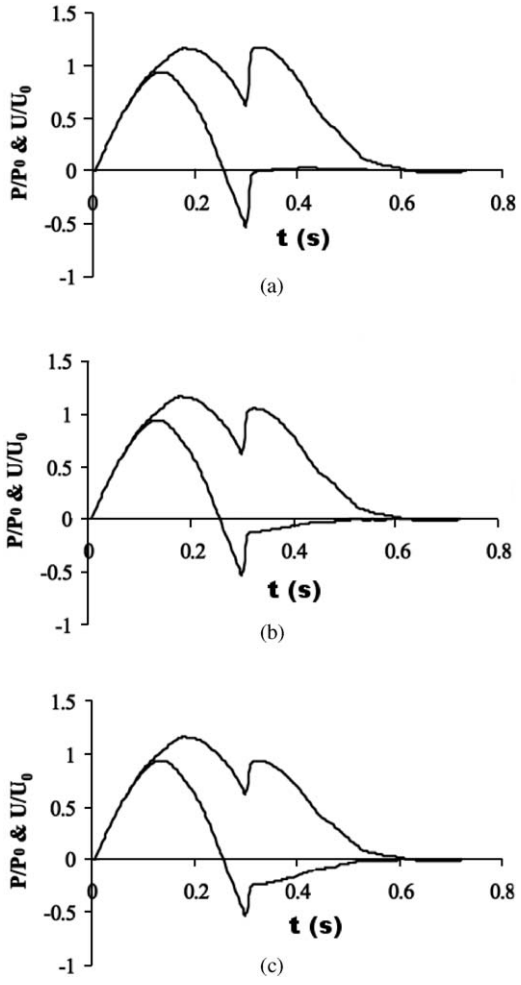

Fig. 8. The pressure (upper) and velocity (lower) waveforms in the ascending aorta calculated assuming that the coronary arteries cause the heart not to be a total reflector after the aortic valve is closed: (a) $R = 1$; (b) $R = 0.8$ and (c) $R = 0.6$.

The overall reflection coefficient of the heart in the diastolic phase is still uncertain. In this simulation, we assumed the reflection coefficient of the heart was 1.0, 0.8 and 0.6 when the valve is closed and zero when the valve is opened. The calculated waveforms in the ascending aorta are shown in Fig. 8. The upper line is the pressure and the lower line is the velocity. All the calculations are normalised by the peak value of the input wave. There are two features of the calculation which should be noted:

(1) The incisura is not very sensitive to the changes of the reflection coefficient of the heart. The pressure in the diastolic phase is the result of the summation of the backward waves and the waves reflected by the heart, which are the only waves influenced by the heart's reflection coefficient.

(2) The inverse flow does not go to zero immediately after the valve closes. The less the heart reflects, the longer it takes for the backward flow to go to zero.

4. Conclusions

Before drawing conclusions about our results, we would like to reiterate that the goal of this study was not to develop a realistic model of arterial pulse waves but to develop a model with which we could explore the influence of wave reflections in the complex geometry of the arteries. With this goal in mind, we have used a realistic model of the large arteries adjusted to ensure that the model bifurcations are well matched for the transmission of forward waves. We have made simplifying assumptions about the nature of the pulse generated by the heart, the nature of the terminal segments of our arterial model and that the non-linear effects of convection and pressure-dependent wave speed are negligible. With these assumptions, it is perhaps surprising that the results of our calculations are so successful in their prediction of so many of the features of the arterial pulse wave. The success of this simple models lead us to believe that reflections within the complex arterial system are primary determinants of arterial haemodynamics.

The method of calculation is based upon the method of characteristics which has the distinct advantage that it provides a general solution of the non-linear, one-dimensional equations for flow in elastic tubes. Neglecting viscous dissipation, this solution says that waves

propagate upstream and downstream without change with speeds $U \pm c$, where c is the local wave speed. In this paper, we have made the linearising assumptions that the blood velocity is small compared with the wave speed so that the waves travel with speeds $\pm c$ and that c does not vary with pressure. When the waves encounter a change in the properties of the vessel, either at a bifurcation or a resistance element used to model the terminal vessels of our model, they are reflected and transmitted with magnitudes determined by a reflection coefficient which depend upon the properties of the vessels at the junction. From measurements of the geometrical and elastic properties of arterial bifurcations, it has been suggested that most arterial junctions are well matched for forward wave transmission so that $R \approx 0$ (Papageorgiou and Jones, 1988; Papageorgiou et al., 1990). A less-well-recognised implication of this observation is that the arterial system is poorly matched for backward waves because a bifurcation well matched in one direction is necessarily ill matched in the other. Simply put, this study is an attempt to explore the results of this simple observation in the complex network of the systemic arteries.

With these linearising assumptions, the transfer function calculated for each arterial segment contains all of the information necessary to determine the response of the arterial system to any ejection pattern produced by the left ventricle. These transfer functions are extremely complex, indicating the complex pattern of reflection and re-reflection produced by the terminal segments and the bifurcations themselves. Comparing the transfer functions at different distances from the heart, we see that there is a kind of 'wave trapping' in the more distal parts of the arterial tree because the bifurcations are poorly matched for backward waves. That is, backward waves reflected by the terminal segments suffer significant re-reflections at each of the bifurcations they encounter and so the wave transmitted back to the heart is greatly diminished. This phenomena can explain why previous studies have found little evidence of disturbances on flow in the ascending aorta resulting from disturbances or even occlusions of peripheral vessels (Peterson and Gerst, 1956; Westerhof et al., 1979; Latham et al., 1985).

The complexity of the transfer functions which we have calculated may also explain why studies based upon the impedance method have been so difficult to interpret when it comes to wave reflections. The transfer function can be used to calculate the response of the arterial model to sinusoidal inputs of different frequencies. We have, in fact, done such calculations but have not reported them here because we did not find the results to be particularly helpful. Like Taylor (1966) in his study of a random bifurcating tree, we could not find any simple way to associate the magnitude and phase of our results with the properties of our arterial model. Our conclusion was that the complexity of the arterial reflections could not be modelled using the concept of a simple 'effective' reflection site.

The results of our calculations suggest that wave propagation in the arterial system is perhaps the dominant factor determining the aortic pressure and velocity waveforms. The tree of waves model gives us a method of tracking the waves generated by the ventricle as they propagate through the arterial system being reflected and re-reflected at each bifurcation. The results of the calculation exhibit most of the features of physiologically measured waveforms, that is somewhat surprising given the number of simplifications which have been made. The tree of waves model also enables us to track the origin of each wave and thus determine the contribution of the different parts of the circulation to the aortic waveforms and to discuss the effects of some pathological conditions.

We conclude by observing that the transfer function could be an important index of the arterial system. Unfortunately, however, measurement of a transfer function is difficult. Sipkema et al. (1980) tried to measure an aortic transfer function in dogs by generating a pulse by rapid clamping of the ascending aorta and measuring the reaction of the system. As far as we know, there have been no attempts to measure an arterial transfer function in humans.

References

Allieve, L., 1909. Allgenmeine Theorie uber die verandliche Bewegung des Wassers in Leitungen. Springer, Berlin.

Anliker, M., Rockwell, R.L., Ogden, E., 1971. Nonlinear analysis of flow pulses and shock waves in arteries, Part 1: derivation and properties of mathematical model. Zeitschrift für Angewandte Mathematik und Physik 22, 217–246.

Avolio, A.P., 1980. A multibranched model of the human arterial system. Medical and Biological Engineering and Computing 18, 709–718.

Avolio, A.P., Nichols, W.W., O'Rourke, M.F., 1984. Propagation of the pressure pulse in the systemic arterial system of the kangaroo. American Journal of Physiology 249, R335–R340.

Davies, R.H., 1994. The analysis of human cardiovascular system using the method of characteristics. Ph.D. Thesis, Imperial College, University of London, London, UK.

Frank, O., 1899. Die grundform des arteriellen pulses. erste abhandlung, mathematische analyse. Zeitschrift fuer Biologie 37, 483–526.

Frank, O., 1905. Der Puls in den Arterien. Zeitschrift fuer Biologie 46, 441–553.

Guyton, A.C., 1981. Textbook of Medical Physiology. W.B. Saunders, Philadelphia.

Hamilton, W.F., 1944. The patterns of the arterial pressure pulse. American Journal of Physiology 141, 235–241.

Hardung, V., 1952. Zur mathematischen behandlung der dampfung und reflection der pulswellen. Archivfuer Kreislaufforschung 18, 167–175.

Jones, C.J.H., Sugawara, M., Davies, R.H., Kondoh, Y., Uchida, K., Parker, K.H., 1994. Arterial wave intensity: physical meaning and physiological significance. In: Hosada, S., Yaganuma, T.,

Sugawara, M., Taylor, M.G., Caro, C.G. (Eds.), Recent Advances in Cardiovascular Mechanics. Harwood Academic Press, New York, pp. 129–148.

Latham, R.D., Westerhof, N., Sipkema, P., Rubal, B., Reuderink, K., 1985. Regional wave travel and reflections along the human aorta: a study with six simultaneous micromanometric pressures. Circulation 72, 1257–1269.

Levick, J.R., 1992. An Introduction to Cardiovascular Physiology. Butterworth-Heinemann, London.

Lighthill, M.J., 1978. Waves in Fluids. Cambridge University Press, Cambridge.

McDonald, D.A., 1974. Blood Flow in Arteries. Camelot Press, Southampton.

Milnor, W.R., 1989. Hemodynamics. Williams and Wilkins, Baltimore, MD.

Murgo, J.P., Westerhof, N., Giolma, J.P., Altobelli, S.A., 1981. Effects of exercise on aortic input impedance and pressure wave forms in normal humans. Circulation Research 3, 334–343.

Nichols, W.W., O'Rourke, M.F., 1998. McDonald's Blood Flow in Arteries: Theoretical, Experimental and Clinical Principles, 4th Edition. Edward Arnold, London.

Nichols, W.W., Avolio, A.P., O'Rourke, M.F., 1986. Ascending aortic impedance patterns in the kangaroo; their explanation and relation to pressure waveforms. Circulation Research 59, 217–255.

O'Rourke, M.F., 1967. Pressure and velocity waves in systemic arteries and the anatomical design of the arterial system. Journal of Applied Physiology 23, 139–149.

O'Rourke, M.F., Avolio, A.P., 1980. Pulsatile flow and pressure in human systemic arteries: studies in man and in a multi-branched model of the human systemic arterial tree. Circulation Research 46, 363–372.

Papageorgiou, G., Jones, N.B., 1988. Wave reflection and hydraulic impedance in the healthy arterial system: a controversial subject. Medical and Biological Engineering and Computing 26, 237–242.

Papageorgiou, G., Jones, N.B., Redding, V.J., Hudson, N., 1990. The area ratio of normal arterial junctions and its implications in pulse wave reflections. Cardiovascular Research 6, 478–484.

Parker, K.H., Jones, C.J.H., 1990. Forward and backward running waves in the arteries: analysis using the method of characteristics. Journal of Biomechanical Engineering 112, 322–326.

Peterson, L.H., Gerst, P.H., 1956. Significance of reflected waves within the arterial system. Federation Proceedings 15 (496), 145.

Sipkema, P., Westerhof, H., Randall, O.X., 1980. The arterial system characterised in the time domain. Cardiovascular Research 14, 270–279.

Skalak, R., 1972. Synthesis of a complete circulation. In: Bergel, D.H. (Ed.), Cardiovascular Fluid Dynamics, Vol. 2. Academic Press, London (Chapter 19).

Stergiopulos, N., Westerhof, N., 1998. Determinants of pulse pressure. Hypertension 32, 556–559.

Stergiopulos, N., Young, D.F., Rogge, T.R., 1992. Computer simulation of arterial flow with applications to arterial and aortic stenoses. Journal of Biomechanics 25, 1477–1488.

Stettler, J.C., Niederer, P., Anliker, M., 1981. Theoretical analysis of arterial hemodynamics including the influence of bifurcations. Part i: mathematical model and prediction of normal pulse pattern. Part ii: critical evaluation of theoretical model and comparison with noninvasive measurements of flow patterns in normal and pathological cases. Annals of Biomedical Engineering 9, 145–164, 165–175.

Taylor, M.G., 1966. The input impedance of an assembly of randomly branching elastic tubes. Biophysical Journal 6, 29–51.

Van den Bos, G.C., Westerhoff, N., Elzinga, G., Sipkema, P., 1971. Reflection in the systemic arterial system: effects of aortic and carotid occlusion. Cardiovascular Research 10, 565–573.

Wang, J.-J., 1997. Wave propagation in a model of the human arterial system. Ph.D. Thesis, Imperial College, University of London, UK.

Westerhof, N., Noordergraaf, A., 1970. Arterial viscoelasticity: a generalized model. Effect on input impedance and wave travel in the systemic tree. Journal of Biomechanics 3, 357–379.

Westerhof, N., Bosman, F., De Vries, C.J., Noordergraaf, A., 1969. Analogue studies of the human systemic arterial tree. Journal of Biomechanics 2, 121–143.

Westerhof, N., Sipkema, P., Van den Bos, G.C., Elzinga, G., 1972. Forward and backward waves in the arterial system. Cardiovascular Research 6, 648–656.

Westerhof, N., Elzinga, G., Van den Bos, G.C., 1973. Influence of central and peripheral changes on the hydraulic input impedance of the systemic arterial tree. Medical and Biological Engineering 11, 710–722.

Westerhof, N., Murgo, J.P., Sipkema, P., Giolma, J.P., Elzinga, G., 1979. Arterial impedance. In: Hwang, N.H.C., Gross, D.R., Patel, D.J. (Eds.), Quantitative Cardiovascular Studies. University Park Press, Baltimore, pp. 111–150.

Zamir, M., 1998. Mechanics of blood supply to the heart: wave reflection effects in a right coronary artery. Proceedings of the Royal Society B 265, 439–444.